

# THE LANCET

## Microbe

### **Supplementary appendix**

This appendix formed part of the original submission and has been peer reviewed. We post it as supplied by the authors.

Supplement to: Schlottau K, Rissmann M, Graaf A, et al. SARS-CoV-2 in fruit bats, ferrets, pigs, and chickens: an experimental transmission study. *Lancet Microbe* 2020; published online July 7. [https://doi.org/10.1016/S2666-5247\(20\)30089-6](https://doi.org/10.1016/S2666-5247(20)30089-6).

## Supplementary

### **Experimental transmission studies of SARS-CoV-2 in fruit bats, ferrets, pigs and chickens**

Kore Schlottau<sup>\*1</sup>, Melanie Rissmann<sup>\*2</sup>, Annika Graaf<sup>\*1</sup>, Jacob Schön<sup>\*1</sup>, Julia Sehl<sup>3</sup>, Claudia Wylezich<sup>1</sup>, Dirk Höper<sup>1</sup>, Thomas C. Mettenleiter<sup>4</sup>, Anne Balkema-Buschmann<sup>±,2</sup>, Timm Harder<sup>±,1</sup>, Christian Grund<sup>±,1</sup>, Donata Hoffmann<sup>±,1</sup>, Angele Breithaupt<sup>#,3</sup> and Martin Beer<sup>#,1</sup>

Supplementary Material & Methods .....	1
Supplementary Tables.....	6
Supplementary Figures.....	10

## **Supplementary Material & Methods**

### **Virus and cells**

SARS-CoV-2 isolate 2019\_nCoV Muc-IMB-1 was kindly provided by German Armed Forces Institute of Microbiology (Munich, Germany). The complete sequence of this isolate is available through GISAID under the accession ID\_EPI\_ISL\_406862 and name “hCoV-19/Germany/BavPat1/2020”. The virus was propagated once in Vero E6 in a mixture of equal volumes of Eagle MEM (Hanks’ balanced salts solution) and Eagle MEM (Earle’s balanced salts solution) supplemented with 2mM L-Glutamine, nonessential amino acids, adjusted to 850 mg/L, NaHCO<sub>3</sub>, 120 mg/L sodium pyruvate, 10% fetal bovine serum (FBS), pH 7.2. No contaminants were detected within the virus stock preparation and the sequence identity of the passaged virus was confirmed by metagenomics analysis employing previously published high throughput sequencing procedures using Illumina MiSeq sequencing (1\*). The virus was harvested after 72h, titrated on Vero E6 cells and stored at -80°C until further use.

### **RNA extraction and detection of SARS-CoV-2**

Total RNA was extracted from oral, nasal and rectal samples, nasal washes, fecal samples and tissue samples collected at different time points using the NucleoMagVet kit (MachereyNagel, Düren, Germany) according to the manufacturer’s instructions. Tissue samples were homogenized in 1 ml cell culture medium and a 5 mm steel bead in a TissueLyser (Qiagen, Hilden, Germany). Fecal samples were vortexed in sterile NaCl and the supernatant was sterile filtered (22 µm) after centrifugation. Swab samples were transferred into 0.5-1 ml of serum-free tissue culture media and further processed after 30 min shaking.

SARS-CoV-2 RNA was detected by the “E-gene Sarbeco FAM” protocol published by Corman et al. (15). The RT-qPCR reaction was prepared using the AgPath-ID-One-Step RT-PCR kit (Thermo Fisher Scientific, Waltham, Massachusetts, USA) in a volume of 12.5 µl including 1 µl of E-gene Sarbeco FAM mix, 1 µl of β-Actin-mix2-HEX as internal control) and 2.5 µl of extracted RNA. The reaction was performed for 10 min at 45°C for reverse transcription, 5 min at 95°C for activation, and 42 cycles of 15 sec at 95°C for denaturation, 20 sec at 57°C for annealing and 30 sec at 72°C for elongation. Fluorescence was measured during the annealing phase. All RT-qPCRs were performed on a BioRad real-time CFX96 detection system (BioRad, Hercules, USA). Absolute quantification was done using a standard quantified by the QX200 Droplet Digital PCR System in combination with the 1-Step RT-ddPCR Advanced Kit for Probes (BioRad, Hercules, USA).

Nasal conchae samples from ferret #1, #2, #3,#4, #10 and #11 were subjected to high-throughput sequencing and viral genomes compared to the inoculum by employing previously published high throughput sequencing procedures using Ion Torrent S5XL instrument (1\*).

#### Detection of SARS-CoV-2 reactive antibodies

Serum samples collected before the start of the experiments as well as on autopsy were tested for the presence of SARS-CoV-2 reactive antibodies by indirect immunofluorescence assay (iIFA) and virus neutralization test (VNT).

Confluent Vero E6 cells in a 96 well plate were infected with 0.1 MOI of SARS-CoV-2 or cell culture medium for negative control cells. After 24h, cells were fixed with 4% paraformaldehyde and permeabilized with 0.5% Triton-X-100. Serum samples were heat inactivated at 56°C for 30 min. For antibody detection, 50 µl of a 2-fold dilution series of the serum samples (starting from 1:20) were added in parallel to the SARS-CoV-2 positive and negative cells. After 1h incubation, cells were washed and incubated for 1h with a goat-anti-ferret-IgG-FITC antibody (1:250, Bethyl, Texas, USA), mouse-anti-bat-IgG #6 (1:100, FLI produced) combined with a goat-anti-mouse-Cy3 (1:400, Jackson Immunoresearch, Pennsylvania, USA), goat-anti-pig-FITC IgG (1:2000, antibodies-online, Aachen, Germany), goat-anti-chicken-IgG-FITC (1:400, OriGene Technologies GmbH, Maryland, USA), respectively. After final washing, cells were analyzed by fluorescence microscopy.

For virus neutralization assay, 50 µl of medium containing  $10^{3.3}$  TCID<sub>50</sub> SARS-CoV-2 were mixed with 50 µl of diluted serum. Each sample was tested in triplicates. After 1h incubation at 37°C the mixture was transferred to confluent Vero E6 cells in a 96 well plate. Viral replication was assessed after 5 days at 37°C, 5% CO<sub>2</sub> by the detection of CPE.

#### Virus titration

Virus titer used for infection experiments was confirmed by titration on Vero E6 cells and evaluation of CPE after 5 days. RT-qPCR positive nasal washes and tissue samples were titrated on Vero E6 cells as well.

#### Pathology: Autopsy, histopathology, immunohistochemistry, in situ hybridization

Full autopsies were performed on all animals according to a standard protocol under BSL3 conditions. The following tissues were collected and fixed in 10% neutral-buffered formalin: Nasal conchae (non-respiratory, respiratory and olfactory region), trachea, lung (inflated with formalin, left and right cranial as well as caudal lobe), tracheobronchial lymph node, heart (left

ventricle), liver, spleen, duodenum, colon, pancreas, kidney, adrenal gland, skeletal muscle, inguinal skin, brain. To avoid cross contamination at autopsy, instruments were washed in sodium hypochlorite-based reagents and water after each tissue sample. Tissues of ferrets and fruit bats were embedded in paraffin, and 3 µm sections were stained with hematoxylin and eosin for light microscopical examination.

For SARS-CoV-2 antigen detection, tissue sections of all bats and ferrets were deparaffinized and rehydrated according to standardized procedures. Antigen heat retrieval was performed (citrate buffer, pH 6, 12 min, microwave 600 Watt). Nonspecific antibody binding was blocked with goat normal serum for 30 min at room temperature. Polyclonal anti-SARS Nucleocapsid antibody (dilution 1:200, Novus Biologicals # NB100-56576, Centennial, CO, USA) was incubated over night at room temperature, followed by washing steps and incubation with a secondary biotinylated goat anti-rabbit antibody (dilution 1:200; Vector Laboratories, Burlingame, CA, USA) for 30 min at room temperature. Freshly prepared avidin-biotin-peroxidase complex (ABC) solution (Vectastain Elite ABC Kit; Vector Laboratories) was applied, and a bright red antigen labelling was produced with the 3-amino-9-ethylcarbazole substrate (AEC, Dako, Agilent, Santa Clara, CA, USA). The sections were counterstained with hematoxylin, rehydrated, and mounted on coverslips. In each run, we included consecutive sections incubated with negative rabbit control serum, historical tissue sections from SARS-CoV-2 negative ferrets and bats (negative control), and sections of cell pellets infected with SARS-CoV-2 and fixed after 24 h (positive control).

To confirm IHC, RNA in situ hybridization (ISH) was performed on tissues of selected animals with RNAScope 2-5 HD Reagent Kit-Red (ACD, Advanced Cell Diagnostics, Newark, CA) according to the manufacturer's instructions. For hybridization, RNAScope® probes were custom designed by ACD for SARS-CoV-2 NSP. The specificity of the probes was verified using a positive control probe peptidylprolyl isomerase B (cyclophilin B, ppib) and a negative control probe dihydrodipicolinate reductase (DapB). Evaluation and interpretation of pathology data were performed by a board-certified pathologist (DiplECVP).

### Susceptibility of different porcine cell lines to SARS-CoV-2

Porcine cell lines, porcine kidney-15 (PK-15), swine kidney-6 (SK-6) and swine testicle (ST) cells that are routinely used for porcine virus isolation attempts at FLI, were investigated for their permissivity to SARS-CoV-2. Cells were maintained in modified Eagle medium (MEM) supplemented with 10% FBS. Nearly confluent cells were infected with SARS-CoV-2 at a titer of  $10^{5.5}$  TCID<sub>50</sub> in a microtitration format in 96well plates as well as T25 cell culture systems

or were mock-infected with medium only. Vero E6 cells were used as a highly permissive control. Cells were observed for cytopathic effects (CPE) daily until six days post infection. Supernatant samples from infected T25 cell culture systems were harvested at 2 and 72 hpi for RT-qPCR analysis (Table S2). In addition, cell free supernatants were used for virus titration on Vero E6 cells (Table S3). At 48 hpi, cells were fixated and stained as described for IFA (Fig. S5). Cell nuclei were labelled with DAPI (invitrogen, Waltham, Massachusetts, USA).

#### Susceptibility of embryonated chicken eggs

Six 9-day-old SPF chicken eggs were inoculated by allantoic sac route, using 0.1 ml with  $5.5 \times 10^4$  TCID<sub>50</sub>. Amniotic-Allantoic fluid (AAF) was harvested after incubation for 7 days and tested by RT-qPCR and virus isolation on Vero E6 cells.

#### Statistical experiment planning

For the calculation of the animal numbers, virus detection was used as the primary endpoint. For the presentation of a possible follow-up concept, the significance level of 5% is applied, and the power should always be  $\geq 80\%$  (error 2. species  $\leq 20\%$ ). A binary target value (virus presence/non-existence) was assumed for this planning. In order to maximize the information gain per animal and the significance of the statistical analysis, it was planned to collect the endpoint virus detection 21 days after inoculation. This will further increase the power of the planned statistical tests. It was assumed that in at least 50% of the animals, the infection is present and therefore virus is detectable. To verify this hypothesis, the one-sided exact binomial test for one sample is used. Under these assumptions, and in view of the fact that this is an exploratory pilot study, only a small number of animals will be sampled. A total of nine to a maximum of 14 animals per animal species are estimated for all experimental procedures explained in detail by the end of the observation period in order to collect the necessary preliminary data for planning a possible follow-up study. For the planned number of animals and assuming a minimum 50% probability of detection, the certainty of detecting at least 1 infected animal over the entire experimental procedure (i.e. virus detection) is always higher than 80%.

#### Further Discussion

In general, RT-qPCR detected viral genome in a significantly broader spectrum of tissues than IHC, which detects cell associated proteins. The differences could be explained by (i) a higher sensitivity of RT-qPCR, (ii) the restriction of labelling to cell associated antigen whereas RT-qPCR detects viral RNA in blood, secretions and excretions (i.e. tracheal and bronchial mucus,

saliva on the fur), and not least (iii) viral antigen was found in restricted foci of the nasal cavity only, that might be missed in tissue sections although several areas have been analyzed. Although less sensitive, IHC is an excellent tool to localize and identify infected target cells. Numerous extraction controls were executed and questionable results were confirmed by a second RT-qPCR assay. Therefore, we assume that our RT-qPCR results are highly reliable.

## References

1\* Wylezich C, Papa A, Beer M, Hoper D. A Versatile Sample Processing Workflow for Metagenomic Pathogen Detection. *Scientific reports*. 2018;8(1):13108.

1 **Supplementary Tables**

2 **Table S1: RT-qPCR Cq values, IHC and ISH tissue results for A) fruit bats and B) ferrets.** The first value is the Cq value, the second the IHC  
 3 result (positive/negative) and the third the ISH results (positive/negative, only performed on selected samples).

A)	cerebellum	cerebrum	nasal conchae	skin	muscle	trachea	lung (left)	lung (right)	lung lymphnode	heart	kidney	adrenal gland	liver	spleen	pancreas	duodendum	colon
fruit bat #1, day 4	-/-	-/	<b>23.16</b> /+/+	-/-	-/-	36.64/-	-/-	-/-	35.62/-	-/-	-/-	-/-	-/-	-/-	-/-	-/-	-/-
fruit bat #2, day 4	-/-/-	-/-/-	<b>31.15</b> /+/+	36.90/-/-	-/-/-	23.88/-/-	36.93/-/-	-/-/-	32.08/-/-	35.28/-/-	-/-/-	35.57/-/-	-/-/-	-/-/-	-/-/-	36.11/-/-	-/-/-
fruit bat #3, day 8	-/-	-/-	38.97/-	-/-	-/-	-/-	-/-	-/-	-/-	-/-	-/-	-/-	-/-	-/-	-/-	33.81/-	-/-
fruit bat #4, day 8	-/-	-/-	-/-	36.27/-	-/-	-/-	-/-	-/-	-/-	-/-	-/-	40.58/-	-/-	-/-	-/-	-/-	-/-
fruit bat #5, day 12	-/-	-/-	28.19/-	-/-	-/-	-/-	-/-	-/-	-/-	-/-	-/-	-/-	-/-	-/-	-/-	-/-	-/-
fruit bat #6, day 12	-/-	-/-	-/-	-/-	-/-	-/-	-/-	-/-	-/-	-/-	-/-	-/-	-/-	-/-	-/-	-/-	-/-
fruit bat #7, day 21	-/-	-/-	28.61/-	-/-	-/-	-/-	-/-	-/-	-/-	-/-	-/-	-/-	-/-	-/-	-/-	-/-	-/-
fruit bat #8, day 21	-/-	-/-	35.45/-	-/-	-/-	-/-	-/-	-/-	-/-	-/-	-/-	-/-	-/-	-/-	-/-	-/-	-/-
fruit bat #9, day 21	-/-	-/-	35.53/-	-/-	-/-	-/-	-/-	-/-	-/-	-/-	-/-	-/-	-/-	-/-	-/-	-/-	-/-
fruit bat #10, day 21	-/-	-/-	32.89/-	-/-	-/-	-/-	-/-	-/-	-/-	-/-	-/-	-/-	-/-	-/-	-/-	-/-	-/-
fruit bat #11, day 21	-/-	-/-	-/-	-/-	-/-	-/-	-/-	-/-	-/-	-/-	-/-	-/-	-/-	-/-	-/-	-/-	-/-
fruit bat #12, day 21	-/-	-/-	-/-	-/-	-/-	-/-	-/-	-/-	-/-	-/-	-/-	-/-	-/-	-/-	-/-	-/-	-/-

4

B)	cerebellum	cerebrum	nasal conchae	skin	muscle	trachea	lung (left)	lung (right)	lung lymphnode	heart	kidney	adrenal gland	liver	spleen	pancreas	duodendum	colon
ferret #1, day 4	-/-/-	-/-/-	<b>24.31</b> /+/+	36.20/-/-	37.18/-/-	35.56/-/-	29.66/-/-	-/-/-	37.12/-/-	-/-/-	-/-/-	-/-/-	-/-/-	-/-/-	-/-/-	-/-/-	37.30/-/-
ferret #2, day 4	-/-	-/-	<b>26.21</b> /+	34.75/-	38.66/-	37.19/-	38.68/-	35.72/-	-/-	-/-	-/-	-/-	-/-	-/-	-/-	-/-	-/-
ferret #3, day 8	-/-	-/-	<b>34.77</b> /+	-/-	-/-	-/-	-/-	-/-	-/-	-/-	-/-	-/-	-/-	-/-	-/-	-/-	-/-
ferret #4, day 8	-/-	36.95/-	21.57/-	-/-	-/-	-/-	-/-	-/-	-/-	-/-	-/-	-/-	-/-	-/-	-/-	-/-	-/-
ferret #5, day 12	-/-	-/-	-/-	-/-	-/-	-/-	-/-	-/-	-/-	-/-	-/-	-/-	-/-	-/-	-/-	-/-	-/-



ferret #6, day 12	-/-	-/-	29.26/-	-/-	-/-	-/-	-/-	-/-	-/-	-/-	-/-	-/-	-/-	-/-	-/-	-/-	-/-
ferret #7, day 21	-/-	37.78/-	-/-	-/-	-/-	-/-	-/-	-/-	-/-	-/-	-/-	-/-	-/-	-/-	-/-	-/-	-/-
ferret #8, day 21	-/-	-/-	-/-	-/-	-/-	-/-	-/-	-/-	-/-	-/-	-/-	-/-	-/-	-/-	-/-	-/-	-/-
ferret #9, day 21	-/-	-/-	-/-	-/-	-/-	-/-	-/-	-/-	-/-	-/-	-/-	-/-	-/-	-/-	-/-	-/-	37.47/-
ferret #10, day 21	35.29/-	36.68/-	<b>27.50/+</b>	38.35/-	35.35/-	32.21/-	37.61/-	-/-	35.62/-	-/-	-/-	-/-	-/-	-/-	-/-	-/-	-/-
ferret #11, day 21	32.06/-	32.74/-	<b>26.29/+</b>	-/-	38.81/-	37.99/-	36.20/-	34.70/-	-/-	-/-	-/-	38.62/-	-/-	-/-	-/-	-/-	-/-
ferret #12, day 21	-/-	-/-	36.51/-	-/-	-/-	-/-	-/-	-/-	-/-	-/-	-/-	-/-	-/-	-/-	-/-	-/-	-/-

5  
6  
7  
8

**Table S2: Histopathologic findings in the lungs of inoculated and contact Egyptian fruit bats and ferrets.** For all animals, the left and right, cranial as well as caudal lung lobes (= 4 in total) were examined. Conventional Gram stain did not detect intralesional bacteria in lungs affected by infiltrates.

	Infiltrates, interstitial, mixed, mild	Infiltrates, perivascular, lymphocytic, mild	Infiltrates, intra alveolar, mixed, minimal	Alveolar macrophages, number increased, minimal
Day 4	Bat#1; 4/4 lobes			Bat#2; 1/4 lobes
	Ferret#2; 1/4 lobes	Ferret#2; 4/4 lobes	Ferret#1, #2; 1/4 lobes	Ferret#1, 2/4 lobes, Ferret#2; 3/4 lobes
Day 8	Bat#4; 1/4 lobes			
	Ferret#3; 3/4 lobes	Ferret#3; 1/4 lobes		Ferret#3, 4; 1/4 lobes
Day 12	Bat#5; 2/4 lobes			
				Ferret#6; 2/4 lobes
Day 21				Bat#7, 8; 1/4 lobes
				Ferret#8; 1/4 lobes
Day 21 Contact	Bat#10; 1/4 lobes	Bat#10; 1/4 lobes		Bat#10; 2/4 lobes, Bat #11; 1/4 lobes
	Ferret#10, 11; 4/4 lobes, Ferret#12, 11; 1/4 lobes	Ferret#10; 3/4 lobes		Ferret#10, 12 3/4 lobes; Ferret#11, 1/4 lobes;

**Table S3: Detection of SARS-CoV-2 RNA in the supernatant of inoculated porcine cell lines.** Viral supernatant samples were harvested at 2 hpi and 72 hpi. Viral loads were determined by RT-qPCR.

Cell line	RT-qPCR (cq value)	
	2 hpi	72 hpi
<b>VeroE6</b>	28.25	11.16
<b>PK-15</b>	27.68	24.24
<b>SK-6</b>	27.05	12.02
<b>ST</b>	27.84	11.23

**Table S4: Viral titers (TCID<sub>50</sub>/ml) of supernatants of three different porcine cell lines inoculated with SARS-CoV-2.** Viral supernatants were harvested 72 hpi and determined by titration on Vero E6 cells.

Cell line	TCID <sub>50</sub> /ml
<b>VeroE6</b>	1.5 x 10 <sup>8</sup>
<b>PK-15</b>	-
<b>SK-6</b>	6.8 x 10 <sup>7</sup>
<b>ST</b>	3.2 x 10 <sup>6</sup>

## Supplementary Figures

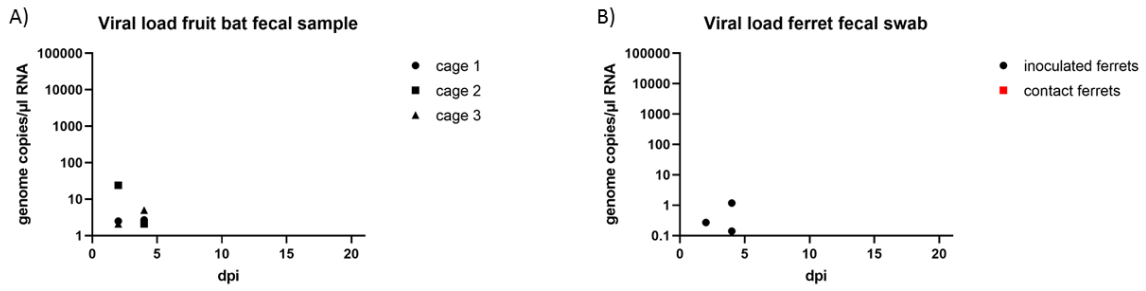


**Figure S1: SARS-CoV-2 viral genome loads over time in A) fecal samples of fruits bats, B) fecal swabs of ferrets.** Genome copies per  $\mu$ l RNA template were calculated based on a quantified standard RNA

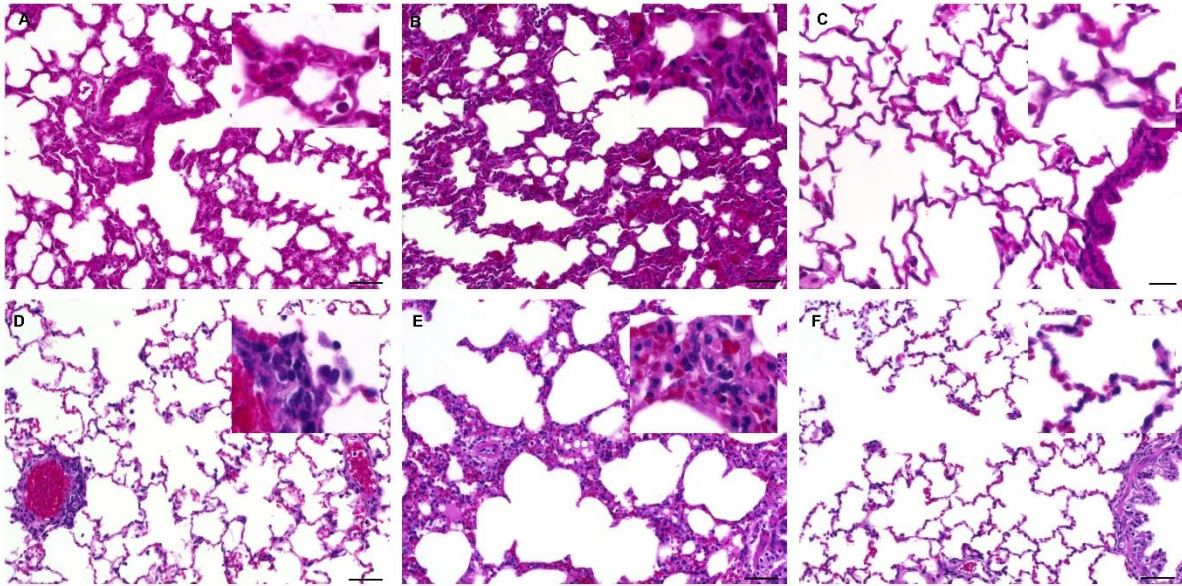


**Figure S2: SARS-CoV-2 associated pulmonary lesions in bats (A-C) and ferrets (D-F).** (A) Thickening of the alveolar wall by congestion and slight, neutrophilic infiltrates, bat, day 4 pi, bar 50  $\mu\text{m}$  (B) Pronounced thickening by congestion and mixed cellular infiltration of the alveolar wall, contact bat, day 21, bar 50  $\mu\text{m}$ , (C) No relevant findings in inoculated bats at day 21 pi, bar 50  $\mu\text{m}$  (D) Perivascular, mononuclear infiltrates, ferret, day 4, bar 50  $\mu\text{m}$ , (E) Thickening by congestion and infiltration of the alveolar wall, contact ferret, day 21, bar 50  $\mu\text{m}$ , (F) No relevant findings in inoculated ferrets at day 21 pi, bar 50  $\mu\text{m}$ .

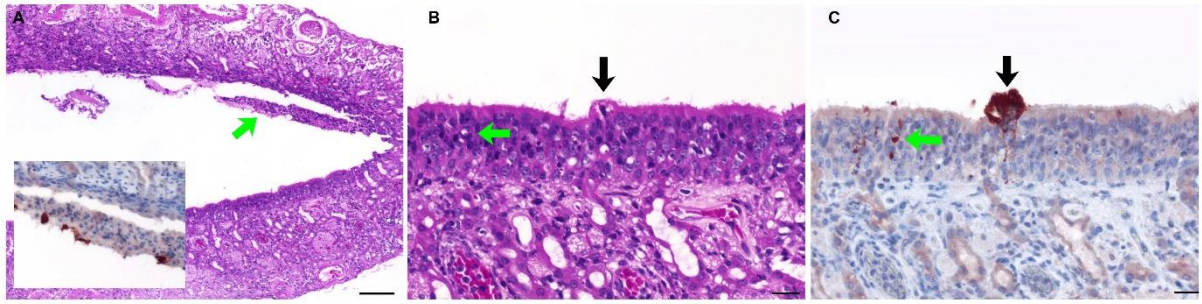


**Figure S3: SARS-CoV-2 in the vomero-nasal organ of a contact ferret on day 21.** (A) Intraluminal debris (green arrow), extensive degeneration, necrosis and focal loss of the olfactory epithelium, abundant mixed cellular infiltrates, intralesional viral antigen (inlay), bar 100  $\mu\text{m}$ , (B) Degeneration with swelling of the olfactory epithelium (black arrow) and apoptosis (green arrow), bar 20  $\mu\text{m}$ , consecutive slide (C) Viral antigen within olfactory epithelium (black and green arrow), bar 20  $\mu\text{m}$ . (A, B) H&E stain, (inlay and C) Immunohistochemistry, ABC Method, AEC chromogen (red-brown), Mayer's hematoxylin counter stain (blue), bar 20  $\mu\text{m}$ .

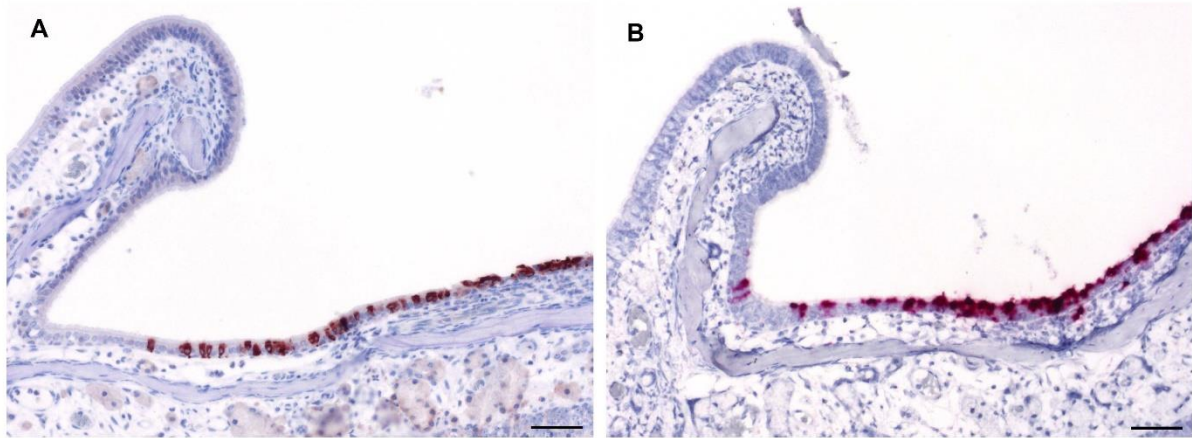


**Figure S4: Comparative SARS-CoV-2 antigen and RNA detection.** Immunohistochemistry and in situ hybridization yielded comparative results with respect to cell types affected and semi-quantitative antigen amount. Exemplarily shown in the respiratory epithelium, ferret, 4 dpi. (A) Immunohistochemistry, ABC Method, AEC chromogen (red-brown), Mayer's hematoxylin counter stain (blue), (B) In situ hybridization, RNAScope®, chromogenic labelling (fast red) with probes to SARS-Cov-2 NSP, Mayer's hematoxylin counter stain (blue).

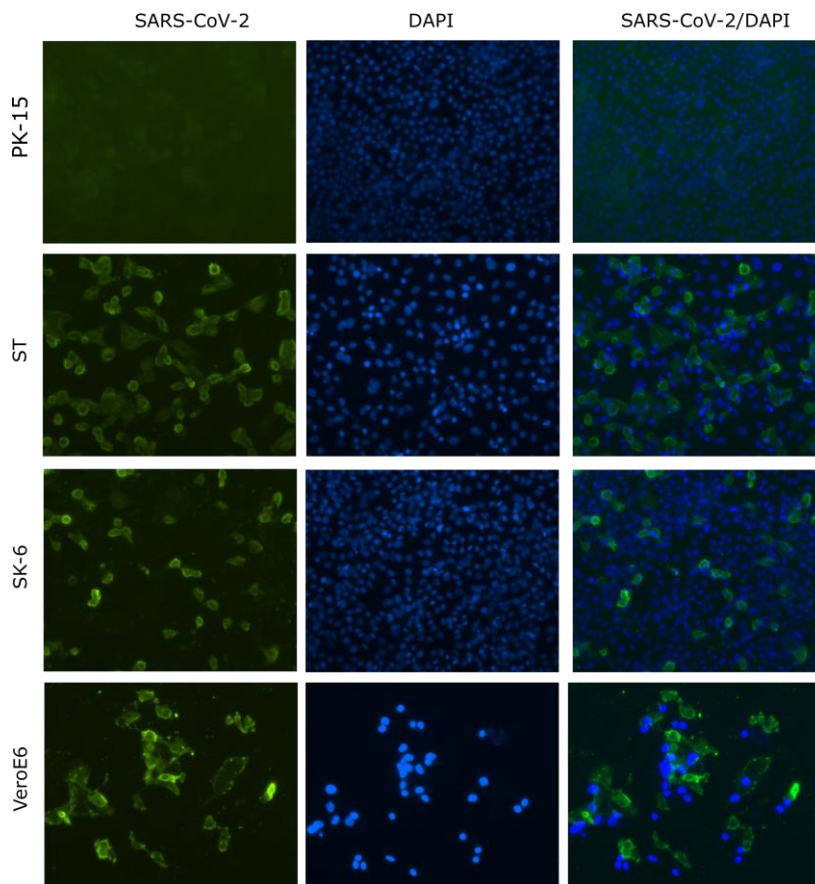


**Figure S5: Antigen expression of SARS-CoV-2 in different porcine cell lines.** SARS-CoV-2 antigen expression was evaluated in three different porcine cell lines (PK-15, ST and SK-6). MOCK-infected cells (of each cell line) were included as negative controls (not shown), and VeroE6 cells as a positive control.